Multi-Core Fiber Backscattered Crosstalk Statistical Distribution Model

Aramais Zakharian and Ming-Jun Li
Corning Incorporated, Corning NY 14831, USA
lim@corning.com

Abstract: Inter-core crosstalk statistical distribution due to Rayleigh backscattering is analyzed for bi-directional transmission in multi-core fibers. The counter-propagating crosstalk distribution is shown to be consistent with a chi-squared statistics with eight degrees of freedom. © 2024 The Author(s)

1. Introduction

The rapid growth of data center traffic volume, and introduction of new communication-intensive applications, drive the demand for optical interconnects with high bandwidth, high spatial density, and low power consumption, making multi-core fibers (MCFs) a compelling candidate for next generation optical fiber links. Inter-core crosstalk is one of the important transmission impairments in uncoupled core MCFs. Due to weak coupling between the cores, it is sensitive to the deployment conditions and perturbations caused by the environmental factors. As such, both the average value and the statistical distribution of the crosstalk must be considered when engineering practical MCF transmission systems.

A significant amount of work has been published to quantify MCF crosstalk dependence on the fiber design parameters and deployment conditions. Theoretical analysis based on both the coupled mode theory (CMT) [1-6] and the coupled power theory (CPT) [7,8] provides consistent results for estimation of crosstalk mean value. The CMT approach also allows evaluation of the crosstalk statistical distribution, which was shown [2,9] in the case of co-propagating main signal and coupled core channels to be represented by a $\chi^2(X,v)$ distribution with v=4 degrees of freedom. The experimentally measured statistical distributions for co-propagating crosstalk, X_{co}, were found to be in good agreement with the theoretical results for various deployment conditions [2,6,9]. Thus, MCF design optimization can be guided by the simulations of crosstalk statistics, relevant for practical transmission systems.

Crosstalk reduction via signal propagation in opposite directions over nearest-neighbor cores of MCF [10-12] is well suited for full duplex transmission systems, as a replacement of optical fiber pairs to implement bidirectional links. The dominant physical mechanisms contributing to the crosstalk $X_{counter}$ in the case of counter-propagating main and coupled core channels, are Rayleigh backscattering and reflection at the connectors, fan-in/fan-out couplers, and at the transceiver [13]. Both the Rayleigh backscattered crosstalk X_b and the reflected crosstalk X_r are significantly smaller than X_{co} due to low levels of light scattering and ≈-40 dB reflection than can be achieved in practice, allowing an increase in MCF core density, compared to unidirectional transmission links. Indirect coupling of X_{co} from nearest-neighbor cores in the interleaved core arrangement can add-up to a similar level of crosstalk as $X_{counter}$, and thus this mechanism must also be considered for bi-directional transmission links. For X_{co} < -35 dB per span, the main component of the counter-propagating crosstalk $X_{counter}$ is due to Rayleigh backscattering [13], and the relation of the mean value of X_b to that of the directly coupled co-propagating crosstalk X_{co} has been previously analyzed [11,14]. However, the statistical distribution for counter-propagating crosstalk has not been reported yet.

In this paper, we apply the CMT to evaluate the statistical distribution of X_b, which is found to follow a probability density function given by a $\chi^2(X,v)$ distribution with twice the number of degrees of freedom, v=8, compared to the distribution of X_{co}. The origin of this difference is attributed to the presence of two different physical paths for backscattered light contribution to X_b.

2. Backscattered crosstalk analysis

We use the crosstalk model based on the CMT, wherein the fiber of length L is represented by a set of uniform segments of length ΔL_i, within each of which the phase and polarization of the electric field are constant, so we can apply the analytic solution for the coupled mode field amplitudes, including the effect of bending and twisting on the mode phase difference between the cores [6]. To represent random perturbations of the MCF refractive index that affect mode phases, we consider random distribution of the fiber segment lengths, and random change of the mode polarization state across segment boundaries. Fig. 1 shows schematically the main signal with power P_0=A_0^2 launched into core 1 and coupled into backward propagating crosstalk in core 2 via two paths: (a) Rayleigh backscattered signal propagating in core 1 and coupling into core 2, resulting in scattered power P_{s2} contribution to X_b; and (b) coupling of the main signal from core 1 into co-propagating crosstalk in core 2, followed by backscattering in core 2, which contributes power P_{2s} to X_b, and P_2 to X_{co}. We note that separate consideration of the two paths for backscattered crosstalk is based on the assumption that recoupling back into the original core can be neglected due to low crosstalk, $P_{2,s2,2s}/P_0 << 1$.

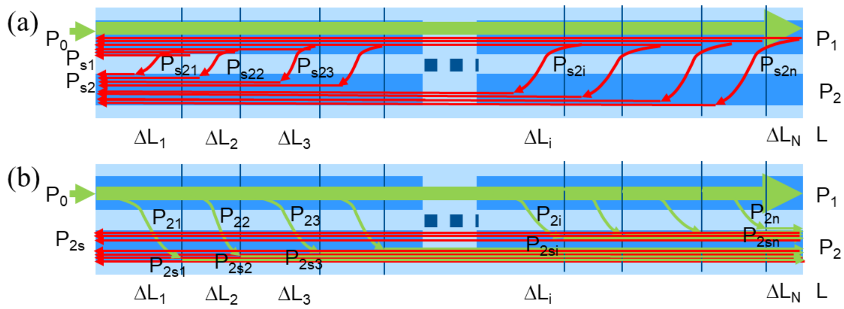

Fig 1. Schematic of Rayleigh backscattered light contribution to the counter-propagating crosstalk in a two core MCF via (a) backscattering of the main signal in core 1 and subsequent coupling into core 2; and (b) coupling of the main signal to core 2, followed by Rayleigh backscattering.

The power P_2 represents the co-propagating component of the crosstalk $X_{co}= P_2(L)/P_1(L)$, where $P_1(z)= P_0 exp(-\alpha z)$ is the power in the MCF core 1, and α is the optical power attenuation coefficient. P_2 can be calculated based on the contribution to the crosstalk from each segment, computed using the CMT [6]:

$$P_2(z) = \sum_{i=1}^{N(z)}\left[\left(\frac{\kappa_i}{g_i}\right)^2 sin^2(g_i\Delta L_i)\right] - \sum_{\substack{i,j=1\\ i\neq j}}^{N(z)}\left[e^{i\frac{1}{2}(\Delta\beta_i\Delta L_i-\Delta\beta_j\Delta L_j)}\frac{\kappa_i\kappa_j}{g_i g_j} sin(g_i\Delta L_i)\, sin(g_j\Delta L_j)\, cos\varphi_{ij}\right] e^{-\alpha z} \quad (1)$$

where κ_i, $\Delta\beta_i$, and ΔL_i are the mode amplitude coupling coefficient, phase difference in propagation constants of the two cores, and the length of segments $i=1\ldots N(z)$ comprising an MCF of length z. The coefficient $g^2=\kappa^2+(\Delta\beta/2)^2$ captures the relative strength of the coupling and phase detuning between the cores, while φ_{ij} is the angle between the electric field polarization in segments i and j. We assume that the attenuation coefficient is substantially the same in both cores, hence X_{co} becomes independent of α. The amount of Rayleigh backscattered power accumulated in core 1 at location z along the fiber length, can be represented as:

$$P_{s1}(z) = \int_z^L \eta P_1(z')dz' = \int_z^L \eta P_0 exp(-\alpha z')dz' = \frac{\eta A_0^2}{\alpha}\left[e^{-\alpha z} - e^{-\alpha L}\right] \quad (2)$$

where $\eta=\alpha_R S_B/2$ is the backscatter factor that depends on the Rayleigh scattering loss coefficient α_R and backscatter capture fraction S_B, defined by the core design [14]. The total backscattered crosstalk power P_{s2} then can be derived analogously to Eq. (1), using Eq. (2):

$$P_{s2}(0) = \frac{\eta A_0^2}{\alpha}\sum_{i=1}^{N}\left\{\left(\frac{\kappa_i}{g_i}\right)^2 sin^2(g_i\Delta L_i)\left[e^{-\alpha z_i} - e^{-\alpha L}\right]\right\} + \frac{\eta A_0^2}{\alpha}\sum_{\substack{i,j=1\\ i\neq j}}^{N}\left\{e^{i\frac{1}{2}(\Delta\beta_i\Delta L_i-\Delta\beta_j\Delta L_j)}\frac{\kappa_i\kappa_j}{g_i g_j} sin(g_i\Delta L_i)\, sin(g_j\Delta L_j) cos\varphi_{ij}\left[e^{-\alpha z_i} - e^{-\alpha L}\right]\right\} \quad (3)$$

Both the first term in Eq. (3), which contributes to determining the average value of the crosstalk, and the second term, that accounts for statistical variations, depend on the attenuation coefficient α. To derive the contribution P_{2s} to X_b, we use Eq. (1) for the coupled power in core 2 to evaluate backscattered power in each fiber segment i, and sum the resulting contributions backpropagated to z=0:

$$P_{2s}(0) = \eta A_0^2\sum_{k=1}^{N}\left\{\sum_{i=1}^{N(z_k)}\left[\left(\frac{\kappa_i}{g_i}\right)^2 sin^2(g_i\Delta L_i)\right]e^{-2\alpha z_k} - \sum_{\substack{i,j=1\\ i\neq j}}^{N(z_k)}\left[e^{i\frac{1}{2}(\Delta\beta_i\Delta L_i-\Delta\beta_j\Delta L_j)}\frac{\kappa_i\kappa_j}{g_i g_j} sin(g_i\Delta L_i)\, sin(g_j\Delta L_j) cos\varphi_{ij}\right]e^{-2\alpha z_k}\right\} \quad (4)$$

From Eqs. (3)-(4) the Raileigh backscattered crosstalk is $X_b=[P_{s2}(0) + P_{2s}(0)]/P_1(L)$ and by taking an ensemble average of X_b over random realizations of segment lengths, the properties of the statistical distribution of the backscattered crosstalk can be determined.

3. Numerical simulation results

We evaluate distribution of X_b numerically for a given MCF core design, geometry, length, and deployment condition using a large number of random realizations of the fiber. To reduce the computational cost due to direct double summation in Eq. (4), we implement it by considering the contribution of the power coupled in segment i from core 1 to core 2 and use analytic integration of the backscattered power from z_i to L in core 2 to include contribution from segments $j > i$, analogous to the integration of the backscattered power in core 1 given by eq. (2).

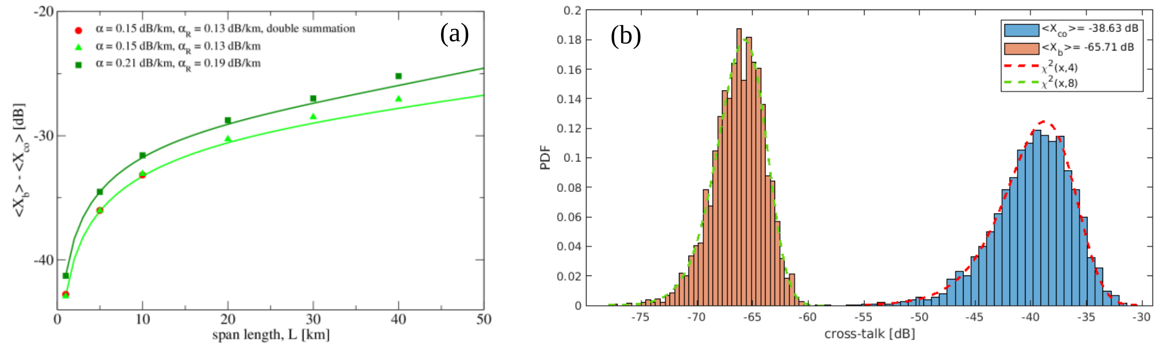

Fig 2. (a) Difference in the mean values of co-propagating and backscattered crosstalk vs span length computed numerically (symbols) vs analytic result (solid lines). (b) Corresponding statistical distributions of the co-propagating and backscattered crosstalk for α=0.15 dB/km, α_R=0.13 dB/km at L=40km. Dashed lines represent single parameter fits of $\chi^2(X,v)$ function to numerical results.

Fig. 2 shows the results of numerical simulations for a 2-core MCF with 45 µm core spacing, coupling coefficient κ=0.007532 m^{-1} at 1550 nm wavelength, and statistical correlation length L_c=0.04 m for exponential distribution function of fiber segment lengths [6]. The fiber with attenuation coefficient α=0.15-0.21 dB/km and Rayleigh scattering loss α_R=0.13-0.19 dB/km is deployed on a D=375 mm diameter spool. The difference between the average values of the co-propagating and backscattered crosstalk is computed using Eq. (4) with double summation (results limited to L<20 km) as well as based on analytic integration of backscattered power, showing full agreement between the two, Fig. 2(a). Good agreement is also obtained with the difference in mean values evaluated based on the analytic approximation given by Eq. (17) in [14]. The numerically computed crosstalk probability density functions are shown in Fig. 2(b) for a span length of 40 km. The co-propagating and backscattered crosstalk distributions are well approximated by $\chi^2(X,v)$ statistical distribution functions with v=4 and v=8, respectively. The doubling of degrees of freedom is due to two channels, P_{s2} and P_{2s}, assumed to be statistically independent in the backscattered crosstalk X_b model. The amplitude, phase and two orthogonal states of polarization in each channel result in a total of eight random variables that contribute to the overall Rayleigh backscattered power. This crosstalk distribution model was found to fit well the numerical results for all simulated span lengths of up to 50 km.

4. Conclusions

Inter-core crosstalk due to Rayleigh backscattering in MCFs designed for bi-directional transmission has been analyzed based on the CMT formulation. Expressions for the crosstalk power coupled to the neighboring core and propagating in the opposite direction have been derived and simplified to allow efficient numerical evaluation. Statistical distribution of the backscattered crosstalk probability density function is found to be consistent with the $\chi^2(X,v)$ distribution with eight degrees of freedom, v=8, due to two different physical paths for backscattered light contribution to X_b. These results allow a more complete characterization of crosstalk for a realistic estimation of crosstalk-induced impairments in bi-directional MCF transmission links.

5. References

[1] J.M. Fini et al., Opt. Express **18**, 15122–15129 (2010)
[2] T. Hayashi et al., Opt. Express **19**, 16576–16592 (2011)
[3] M.-J. Li et al., Proc. OFC, W2A.35 (2015)
[4] C. Antonelli et al., Opt. Exp. **28** 12847–12861 (2020)
[5] A.V.P. Cartaxo et al., J. Light. Technol. **39**, 1830–1842 (2021)
[6] K. Ng et al., Photonics **10** 174 (2023)
[7] M. Koshiba, et al., Opt. Express **19** B102–B111 (2011)
[8] M. Koshiba, et al., IEEE Photonics J. **4** 1987–1995 (2012)
[9] T.M.F. Alves et al., IEEE Phot. Tech. Lett. **31**(8) 651 (2019)
[10] T. Ito et al., Proc. OFC, OTh3K.2 (2013)
[11] A. Sano et al., J. Lightw, Tech. **32**(16), 2771–2779 (2014)
[12] Y. Geng et al., Proc. SPIE, **9390** 939009 (2015)
[13] T. Hayashi et al., Proc. OFC, M1E.1 (2022)
[14] T. Hayashi et al., Optics Express, **30**(13) 23943 (2022)